Journal of Sound and Vibration (1998) **212**(3), 383–394

THE THREE-DIMENSIONAL DtN FINITE ELEMENT METHOD FOR RADIATION PROBLEMS OF THE HELMHOLTZ EQUATION

D. GILJOHANN AND M. BITTNER

TU Darmstadt, *Fachgebiet Maschinenelemente und Maschinenakustik*, *Magdalenenstr*. 4, 64289 *Darmstadt*, *Germany*

(*Received* 22 *May* 1996, *and in final form* 23 *April* 1997)

A finite element method is presented for solving three-dimensional radiation problems in time-harmonic acoustics. This is done by introducing a so-called "Dirichlet-to-Neumann" boundary condition on the outer boundary of the domain discretized with finite elements. This DtN boundary condition is an exact non-reflecting boundary condition. It has been developed by Givoli and Keller [1, 2] for two and three dimensions. Calculations, however, have been carried out only for simple two-dimensional cases [2–6]. In this paper, the Dirichlet-to-Neumann boundary condition for problems in three dimensions is dealt with. From the strong form given by Givoli and Keller, the weak form is derived. Numerical examples show the applicability and performance of the DtN boundary condition.

1. INTRODUCTION

Various problems in applied mechanics and engineering cannot be solved analytically. Therefore, numerical methods have been developed. Two outstanding numerical methods are the boundary element method and the finite element method. The boundary element method (BEM) is a boundary discretization method and hence presents an efficient tool for solving radiation problems in unbounded domains. However, the method fails at so-called "critical frequencies", as weak singular boundary integrals occur. This disadvantage does not appear when the finite element method is used. As the finite element is a domain discretization method, it is actually not appropriate for solving problems in infinite domains. To meet this difficulty, special features can be introduced in order to be able to deal with problems in unbounded domains.

Bettess [7, 8] has developed the theory of semi-infinite elements. A layer of semi-infinite elements is positioned around a finite domain discretized with finite elements. The semi-infinite elements cover the entire unbounded outer domain. In this manner, problems in infinite domains can be solved via the finite element method.

Another approach is to introduce a boundary condition on the outer boundary of the computational domain. This boundary condition has to simulate the infinite outer domain: i.e., it represents the influence of the unbounded domain on the finite domain discretized with finite elements. Givoli and Keller [1, 2] have developed a so-called "Dirichlet-to-Neumann" boundary condition for solving problems in infinite domains. This boundary condition is an exact non-local boundary condition which is non-reflecting: i.e., there are no spurious reflections of waves. Givoli demonstrated its efficiency and performance by several numerical examples for simple radiation problems in two dimensions.

0022–460X/98/180383 + 12 $25.00/0/sv971338

This paper is concerned with solving the three-dimensional radiation problem by using the finite element method and the DtN boundary condition. Initially, the radiation problem is described. Next, the weak form of the DtN boundary condition for the three-dimensional case is derived. Finally, numerical examples are dealt with. By calculating the radiation problem of a breathing sphere, the numerical solution can be compared with the exact solution. Hence the prerequisites are found for using the method in more complicated applications. A comparison between the numerical solution and experimental data shows the performance of the DtN method for a gearbox as an example of a real structure.

2. THE RADIATION PROBLEM

The governing equation for the radiation of acoustic waves is the reduced wave equation, or Helmholtz equation,

$$\Delta\Phi + k^2\Phi = q, \tag{1}$$

where Φ is the complex velocity potential, k is the wavenumber and q is the source term of the potential. The reduced wave equation is derived from the acoustic wave equation when only time harmonic waves are considered [9]. The surface of the radiator presents the inner boundary of the domain. Here two boundary conditions are possible. The Dirichlet boundary condition

$$\Phi = \hat{p}(\mathbf{x})/\mathrm{i}\rho_0 ck, \qquad \forall \mathbf{x} \in \Gamma_p, \tag{2}$$

relates the velocity potential to the sound pressure $\hat{p}(\mathbf{x})$, the sound speed c, the wave number k and the density ρ_0 of the undisturbed medium. i is the imaginary unit and Γ_p is the part of the boundary where the pressure $\hat{p}(\mathbf{x})$ is given (see Figure 1). The Neumann boundary condition

$$\nabla\Phi \cdot \mathbf{n} = -\hat{v}_n(\mathbf{x}), \qquad \forall \mathbf{x} \in \Gamma_v, \tag{3}$$

is a relation between the normal derivative of the potential Φ and the given normal surface velocity $\hat{v}_n$ on the boundary Γ_v. To ensure that there are no incoming waves, the Sommerfeld radiation condition has to be fulfilled. It states that

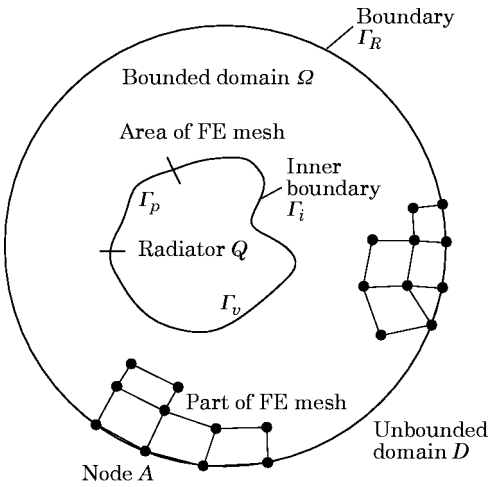

Figure 1. The area Ω of an acoustic radiator with its boundaries Γ_v and Γ_p.

$$\lim_{r\to\infty} r(\partial\Phi/\partial r - ik\Phi) = 0, \tag{4}$$

where r is the radial co-ordinate.

3. THE DtN METHOD

3.1. FINITE ELEMENT FORMULATION

This paper is concerned with the radiation problem in an infinite domain, described by equations (1)–(4). To solve this problem, the unbounded domain is divided into two subdomains by an artificial boundary Γ_R (see Figure 1). For this boundary, a sphere of radius R is chosen. As the original domain is split, the original problem has to be replaced by two sub-problems that have to be solved. They are called sub-problem O and sub-problem I.

Sub-problem O is situated on the outer domain D, which is an infinite domain. It is the radiation problem of a sphere and it is given by equations (1) and (4) and a boundary condition on the inner boundary Γ_R of this sub-problem; namely, the surface of the sphere. For this problem an exact solution can be given. There are, however, unknown constants a_{jn} and b_{jn} (see below), as the boundary condition on the inner boundary Γ_R is not yet known.

According to Smirnow [10], the exact solution of problem O in spherical co-ordinates yields

$$\Phi(r, \theta, \phi) = \sum_{n=0}^{\infty} \frac{\mathrm{H}^{(1)}_{n+1/2}(kr)}{\sqrt{kr}} {\sum_{j=0}^{n}}' \mathrm{P}^j_n(\cos\phi)\,[a_{jn}\sin(j\theta) + b_{jn}\cos(j\theta)], \tag{5}$$

where the unknown constants are determined by

$$a_{jn} = \frac{\sqrt{kR}(2n+1)\,(n-j)!}{2\pi R^2 \mathrm{H}^{(1)}_{n+1/2}(kR)\,(n+j)!} \int_{\Gamma_R} \mathrm{P}^j_n(\cos\varphi)\sin(j\vartheta)\Phi(R, \varphi, \vartheta)\,\mathrm{d}\Gamma, \tag{6}$$

$$b_{jn} = \frac{\sqrt{kR}(2n+1)\,(n-j)!}{2\pi R^2 \mathrm{H}^{(1)}_{n+1/2}(kR)\,(n+j)!} \int_{\Gamma_R} \mathrm{P}^j_n(\cos\varphi)\cos(j\vartheta)\Phi(R, \varphi, \vartheta)\,\mathrm{d}\Gamma. \tag{6}$$

Here $\Phi(R, \varphi, \vartheta)$ is the unknown value of the function Φ on the inner boundary Γ_R. The prime after the sum indicates that the term with $n = 0$ is multiplied by a factor of $1/2$. $\mathrm{H}^{(1)}_n$ is the Hankel function of the first kind and of order $n + 1/2$; P^j_n is the associated Legendre function of the first kind.

Sub-problem I is situated on the inner domain Ω, which is finite. It is the radiation problem of an arbitrary radiator into a domain the outer boundary of which is a sphere. The inner boundary of this sub-problem is the surface of the radiator. The latter is divided into two parts, Γ_p and Γ_v. On the surface Γ_p, the Dirichlet boundary condition is given; and on the surface Γ_v, the Neumann condition holds. The outer boundary is the surface of the sphere Γ_R.

As the domain Ω is finite, the problem can be solved with the help of the finite element method. The strong form of problem I is given by equations (1)–(3) and a boundary condition on the outer boundary Γ_R, which is not yet known. The weak form can be obtained by multiplication with a test function w and integration over the domain Ω. Using Green's formula yields

$$\int_{\Omega} (k^2 w\Phi - \nabla w \cdot \nabla\Phi)\,\mathrm{d}\Omega + \int_{\Gamma_R} w\,\frac{\partial\Phi}{\partial n}\,\mathrm{d}\Gamma = \int_{\Omega} qw\,\mathrm{d}\Omega + \int_{\Gamma_v} w\hat{v}_n\,\mathrm{d}\Gamma, \tag{8}$$

with

$$w(\mathbf{x}) = 0, \qquad q(\mathbf{x}) = (k/\mathrm{i}\rho_0 c)\hat{p}(\mathbf{x}), \qquad \forall \mathbf{x} \in \Gamma_p. \tag{9}$$

In equation (8), the normal derivative of the potential $\partial\Phi/\partial n$ on the outer boundary is not known.

The main problem at this stage is to calculate the integral $\int_{\Gamma_R} w\,\partial\Phi/\partial n\,\mathrm{d}\Gamma$. It can be solved by finding a relation that replaces the value of the outward normal derivative $\partial\Phi/\partial n$ by the value of Φ on the outer boundary Γ_R. This relation can be obtained by problem O.

As mentioned above, it is possible to solve problem O analytically. This gives the unknown function Φ up to the unknown constants (6) and (7). From this, the normal derivative of Φ can be determined, again with these constants. By eliminating the constants of the two relations, one exact relation between the unknown function Φ and its outward normal derivative $\partial\Phi/\partial n$ can be found. This is the so-called "Dirichlet-to-Neumann" condition. It relates the "Dirichlet-datum" Φ to the "Neumann-datum" $\partial\Phi/\partial n$ with the help of an integral operator M:

$$\partial\Phi/\partial n = M\Phi(\mathbf{x}). \tag{10}$$

The DtN condition is chosen as the boundary condition of the outer boundary Γ_R of subproblem I. Hence, the above-mentioned integration can be carried out.

In this manner, the original radiation problem in an unbounded domain given by equations (1)–(4) is replaced by a new problem. The new problem is subproblem I with an exact boundary condition for the outer boundary Γ_R, which can be derived from subproblem O. It is given by equations (1)–(3) and equation (10). As the DtN boundary condition on the sphere contains the exact solution of subproblem O, it is guaranteed that the Sommerfeld radiation condition is fulfilled: i.e., there are no reflected waves.

The following sections are restricted to the most important relations concerning the finite element formulation. For a detailed discussion, refer to standard textbooks such as references [11], [12] and to reference [13]. The finite element formulation results in a system of linear equations,

$$\mathbf{K\Phi} = \mathbf{F}, \tag{11}$$

where $\mathbf{\Phi}$ is the vector of the unknown nodal values of the velocity potential, $\mathbf{K}$ is the stiffness matrix and the vector $\mathbf{F}$ contains the values of the source term. According to Givoli and Keller [1, 2] the stiffness matrix $\mathbf{K}$ consists of two matrices:

$$\mathbf{K} = \mathbf{K}^a + \mathbf{K}^b. \tag{12}$$

$\mathbf{K}^a$ is derived from the domain integral over Ω on the left side of equation (8). $\mathbf{K}^b$ contains the operator M and thus corresponds to the DtN boundary condition

$$K^{\mathrm{b}}_{jl} = \int_{\Gamma_R} N_j(\mathbf{x}) M N_l(\mathbf{x})\,\mathrm{d}\Gamma. \tag{13}$$

In equation (13) $N_j(\mathbf{x})$ is the shape function of the node belonging to equation number j of the resulting system of equations (11). After having solved the set of linear equations (11), the solution of problem O can be obtained with the help of equations (5)–(7). It was shown by Astley [14] that the solution on the outer domain D is identical to that of a concurrent numerical method, the FE mode-matching scheme.

3.2. WEAK FORM OF DtN BOUNDARY CONDITION

Upon the normal derivative of equation (5), the weak form of the DtN boundary condition is obtained:

$$\left.\frac{\partial \Phi(r,\theta,\phi)}{\partial n}\right|_{r=R} = \left.\frac{\partial \Phi(r,\theta,\phi)}{\partial r}\right|_{r=R} = \frac{1}{2\pi R^3} \sum_{n=0}^{\infty} {\sum_{j=0}^{n}}' \beta_{jn} \times \int_{\Gamma_R} \mathrm{P}_n^j(\cos\varphi)\mathrm{P}_n^j(\cos\phi)\cos(j[\theta-\vartheta])\Phi(R,\varphi,\vartheta)\,\mathrm{d}\Gamma, \tag{14}$$

with

$$\beta_{jn} = \frac{(2n+1)(n-j)!}{(n+j)!}\frac{kR\mathrm{H}_{n-1/2}^{(1)}(kR) - (n+1)\mathrm{H}_{n+1/2}^{(1)}(kR)}{\mathrm{H}_{n+1/2}^{(1)}(kR)}. \tag{15}$$

By inserting equation (14) into equation (13) the elements of the stiffness matrix can be determined as

$$\mathrm{K}_{AB}^{\mathrm{b}} = \int_{\Gamma_R} \{N_A(\phi,\theta)\frac{1}{2\pi R}\sum_{n=0}^{\infty}{\sum_{j=0}^{n}}'\beta_{jn} \times \int_{\Gamma_R} \mathrm{P}_n^j(\cos\varphi)\mathrm{P}_n^j(\cos\phi)\cos(j[\theta-\vartheta])N_B(\varphi,\vartheta)\,\mathrm{d}\mathscr{B}\}\,\mathrm{d}\Gamma. \tag{16}$$

$\mathrm{d}\mathscr{B}$ and $\mathrm{d}\Gamma$ indicate the integration over domain Γ_R. Applying an addition theorem for the trigonometric functions and putting the sum in front of the integrals yields

$$K_{AB}^{\mathrm{b}} = \frac{1}{2\pi R^3}\sum_{n=0}^{\infty}{\sum_{j=0}^{n}}'\beta_{jn}\int_{\Gamma_R}\int_{\Gamma_R}\mathrm{P}_n^j(\cos\varphi)\mathrm{P}_n^j(\cos\phi)\,[\cos(j\theta)\cos(j\vartheta) + \sin(j\theta)\sin(j\vartheta)]N_A(\phi,\theta)N_B(\varphi,\vartheta)\,\mathrm{d}\mathscr{B}\,\mathrm{d}\Gamma. \tag{17}$$

It is possible to reduce the interlocked double integrals to only one integral. With the help of the substitution $\mathrm{d}\mathscr{B} = R^2\sin\varphi\,\mathrm{d}\varphi\,\mathrm{d}\vartheta$ the integration over Γ_R in spherical coordinates is performed:

$$K_{AB}^{\mathrm{b}} = \frac{R}{2\pi}\sum_{n=0}^{\infty}{\sum_{j=0}^{n}}'\beta_{jn}\int_{\theta=0}^{2\pi}\int_{\phi=0}^{\pi}\Big\{N_A(\phi,\theta)\mathrm{P}_n^j(\cos\phi)\sin\phi\cos(j\theta) \times \int_{\vartheta=0}^{2\pi}\int_{\varphi=0}^{\pi}\mathrm{P}_n^j(\cos\varphi)\cos(j\vartheta)N_B(\varphi,\vartheta)\sin\varphi\,\mathrm{d}\varphi\,\mathrm{d}\vartheta + N_A(\phi,\theta)\mathrm{P}_n^j(\cos\phi)\sin\phi\sin(j\theta) \times \int_{\vartheta=0}^{2\pi}\int_{\varphi=0}^{\pi}\mathrm{P}_n^j(\cos\varphi)\sin(j\vartheta)N_B(\varphi,\vartheta)\sin\varphi\,\mathrm{d}\varphi\,\mathrm{d}\vartheta\Big\}\,\mathrm{d}\phi\,\mathrm{d}\theta. \tag{18}$$

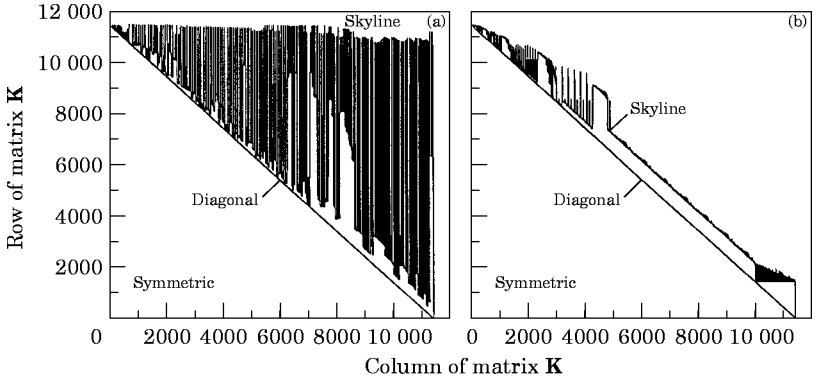

Figure 2. The skyline of the finite element matrix (a) before and (b) after a profile optimization.

With the abbreviations

$$I_{cjnB} := R^2 \int_{\vartheta=0}^{2\pi} \int_{\varphi=0}^{\pi} \mathrm{P}_n^j(\cos\varphi) \cos(j\vartheta) N_B(\varphi, \vartheta) \sin\varphi \, \mathrm{d}\varphi \, \mathrm{d}\vartheta, \tag{19}$$

$$I_{sjnB} := R^2 \int_{\vartheta=0}^{2\pi} \int_{\varphi=0}^{\pi} \mathrm{P}_n^j(\cos\varphi) \sin(j\vartheta) N_B(\varphi, \vartheta) \sin\varphi \, \mathrm{d}\varphi \, \mathrm{d}\vartheta, \tag{20}$$

the DtN elements of the stiffness matrix are finally obtained as

$$K_{AB}^{\mathrm{b}} = \frac{1}{2\pi R^3} \sum_{n=0}^{\infty} {\sum_{j=0}^{n}}' \beta_{jn} (I_{cjnA} I_{cjnB} + I_{sjnA} I_{sjnB}). \tag{21}$$

The computing time evaluating the integrals of equation (21) is negligible, because only surface integrals have to be calculated. When analyzing the acoustic behavior of a structure for several frequencies, the integration does not depend on the frequency. This is in contrast to the BEM ([15, 16]) where the surface integrals usually have to be recalculated for each frequency.

4. EFFECT OF NON-LOCALITY ON SKYLINE OPTIMIZATION

The DtN boundary condition is non-local. This means that the elements K_{AB}^{b} of equation (21) are non-zero even for nodes A and B of other boundary that do not belong to the same element. This spoils the sparseness of the resulting matrix **K**. A bandwidth and profile reduction method given by Hoit and Wilson [17] was used in reference [18] to re-establish a sparse finite element matrix. Before calling the optimization module of the finite element program, a virtual element, which consists of all the nodes of the outer boundary, is added to the finite element model of 11458 degrees of freedom. After profile optimization of the model, this virtual element is removed again. A comparison of the resulting skyline without and after the optimization is shown in Figure 2. The figure shows that despite the non-locality of the DtN boundary condition, the sparseness of the matrix **K** is recovered. The additional storage required due to the DtN boundary condition is negligible.

5. NUMERICAL EXAMPLES

The present finite element formulation has been implemented into the general purpose finite element code FEAP [12]. In what follows, two applications are dealt with.

5.1. RADIATION OF A BREATHING SPHERE

A breathing sphere of a given radius a is the most simple radiating structure. Its velocity potential is calculated as

$$\frac{\Phi(r)}{\Phi_0} := \frac{\Phi(r)}{v_0\, a} = \frac{1}{1 + \mathrm{i}ka}\,\frac{a}{r}\,\mathrm{e}^{\mathrm{i}k(a-r)}, \tag{22}$$

when the Neumann boundary condition v_0 is given on the surface of the sphere. Φ_0 is a reference value.

The stiffness matrix $\mathbf{K}^{\mathrm{b}}$ in equation (21) contains series which have an infinite number of summands. In reality, only a finite number of summands can be calculated. The smaller the number of summands is, the less accurate the numerical solution will be. It is therefore imperative to know how many summands are necessary to obtain an acceptably accurate solution. In the following, the number of summands for calculating the stiffness matrix $\mathbf{K}^{\mathrm{b}}$ is investigated. It is called n_{DtN}. This is done for eight-node three-linear elements and 27-node three-quadratic elements. The potential Φ calculated with eight-node elements is shown in Figure 3, while the potential Φ calculated with 27-node elements is shown in Figure 4. In this particular example, the dimensionless wavernumber ka is chosen to be $ka = 100$. In order to reduce the physical memory requirements and the number of multiplications, R/a is chosen to be $R/a = 1{\cdot}1$. As soon as the finite element solution on Γ_R is known, the potential $\Phi(r_0)$, $r_0 > R$, in the outer domain can be computed by using equations (5)–(7). To integrate the terms (19) and (20), it is sufficient to use five Gaussian points per direction and per surface element on Γ_R.

Finite element calculations have been carried out for different values of n_{DtN}. As expected the results are greatly affected by n_{DtN}. When eight-node elements are used, n_{DtN} must be quite large in order to approximate the solution well; for 27-node elements, n_{DtN} is considerably smaller. Harari and Hughes [4] stated that for two dimensions n_{DtN} has to

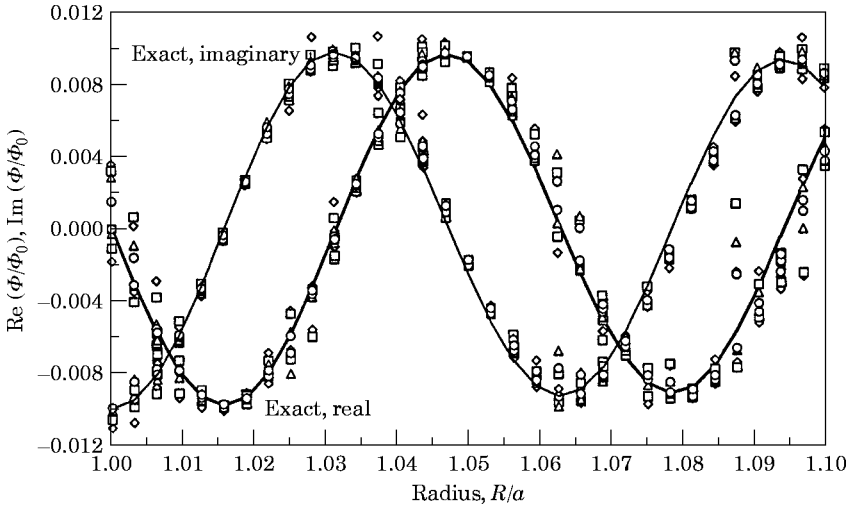

Figure 3. The potential Φ/Φ_0 of a radiating sphere of order zero; $R/a = 1{\cdot}1$, $ka = 100$; variation of order n_{DtN}, eight-node three linear elements. n_{DtN} values: ◇, 10; □, 15; △, 20; ○, 25.

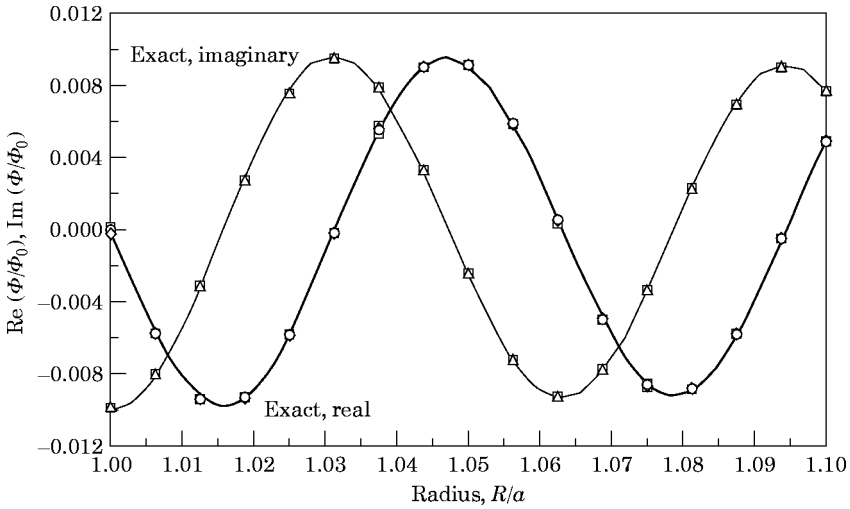

Figure 4. As Figure 3, but 27-node three quadratic elemtents. n_{DtN} values; ◇, 3; □, 10; △, 15; ○, 20.

be greater than kR in order to obtain a good approximation of the solution. The assumption of Harari and Hughes, however, does not hold for the three-dimensional problem. Calculations for various wavenumbers have shown that $n_{\mathrm{DtN}} = 20$ is sufficient to approximate the solution well when 27-node elements are used. This means that in our case n_{DtN} is much smaller than kR, which is $kR = 110$.

Giljohann [18] compared the DtN method with calculations using finite and semi-infinite elements. The computational effort of the DtN method is smaller because the method of the semi-infinite elements always needs a discretization of the far field. Despite the smaller bandwidth of the resulting equations, the infinite elements need more computing time because of their additional nodes and elements; in contrast to the DtN method, which needs only a near field discretization. Although the method of infinite elements uses an approximation for the far field behaviour and special integration procedures for the integration in the infinite direction [19], the accuracy achieved is as good as the results of the DtN method.

5.2. RADIATION OF A GEARBOX

To illustrate the performance and ability of the DtN method for a real structure, the radiation problem on the exterior domain of a gearbox is dealt with. For this purpose, the sound intensity **I** and the radiated power P determined by experiment and by calculation are compared.

First, the experiment is described. The surface of the gearbox is shown in Figure 5. It is excited by an impact hammer. At all the nodes of the surface elements the normal surface velocity $\hat{v}_n$ of the gearbox is measured with accelerometers and then transformed into the frequency domain by a signal analyzer. The averaged squared normal velocity $\bar{v}$,

$$\bar{v} = \frac{1}{\Gamma_v} \int_{\Gamma_v} |\hat{v}_n|^2 \, \mathrm{d}\Gamma, \tag{23}$$

is calculated in the frequency band from 1000 Hz up to 4000 Hz. This is done in order to select those frequencies for the finite element simulations which show a relative maximum of $\bar{v}$, because these frequencies mainly affect the radiation of sound. They are marked in Figure 6.

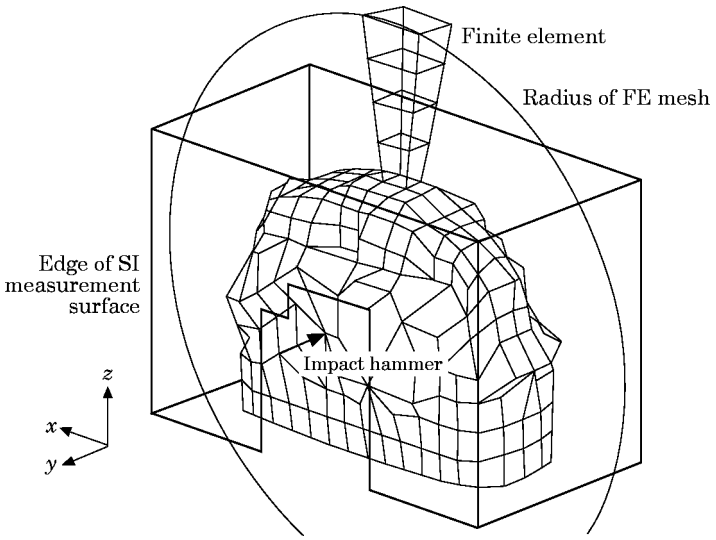

Figure 5. Surface discretization, measurement planes, mesh-generation for the radiation problem and impact hammer.

The active sound intensity **I** is the negative rate of flow of sound energy per unit area, and it is calculated by

$$\mathbf{I}(f) = -\frac{1}{2\pi f \rho_0} \operatorname{Im}\{p(f)\nabla p(f)\} \tag{24}$$

where f is the frequency. The measurement of **I** is carried out in an anechoic chamber. A robot positions a three-dimensonal microphone probe in 359 positions to measure the sound pressure. From this, the sound intensity vectors on the measurement surface are determined according to equation (24).

The radiated power P is calculated according to

$$P(f) = -\int_{\Gamma_I} \mathbf{I}(f) \cdot \mathbf{n}\, \mathrm{d}\Gamma, \tag{25}$$

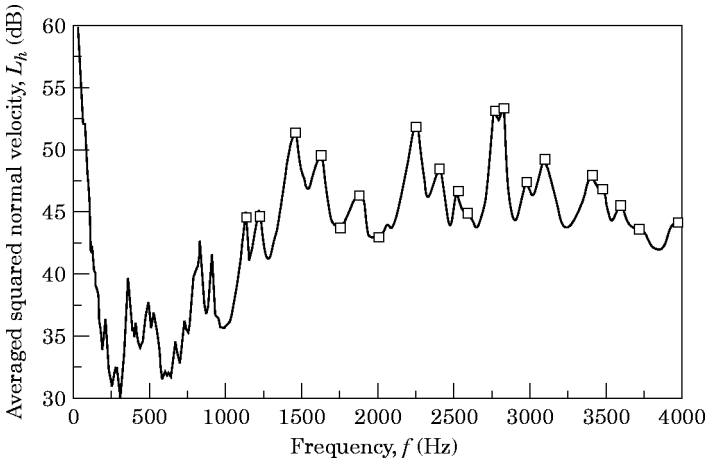

Figure 6. The averaged squared normal velocity. —, Experiment; □, frequencies of simulation.

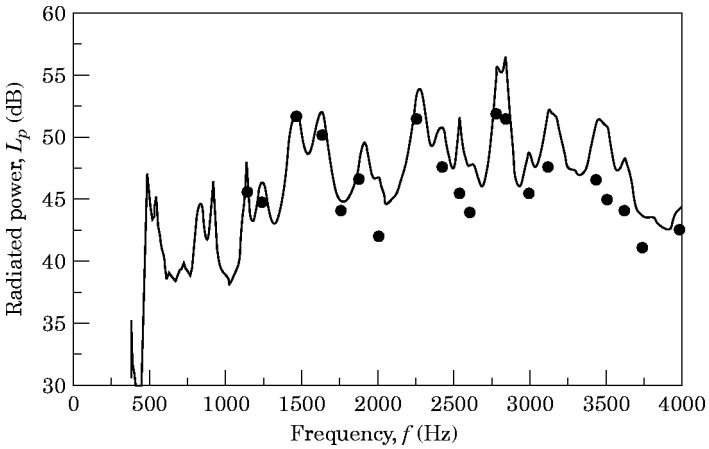

Figure 7. The radiated power level. —, Experiment; ●, DtN–FEM.

where Γ_I is the surface on which the sound intensity is measured. The gap in Γ_I is due to the gear's shafts which penetrate the measurement surface.

For the calculations the exterior domain of the gearbox is discretized by sweeping the surface elements through space radially outward from the gearbox (see Figure 5). The outer border of the finite element discretization of spherical form is determined by the minimal radius which encloses the measurement surface. The resulting finite element mesh with three-linear hexahedral elements consists of 8748 nodes and 8372 finite elements. After calculating the sound intensity an integration of the normal intensity, pointed out in equation (25), is performed. The integration area Γ is selected to be the surface of the gearbox.

The results for the measured and calculated power can be seen in Figure 7. The difference between simulation and experiment is at most 6 dB, which is nearly the same as for calculations carried out with semi-infinite elements by Giljohann and Zopp [20].

One frequency that shows a negligible difference of radiated power is picked out for the plots concerning the spatial distribution of sound intensity (see Figure 8). The directions of the vectors as well as the spatial distribution of maximum and minimum values show

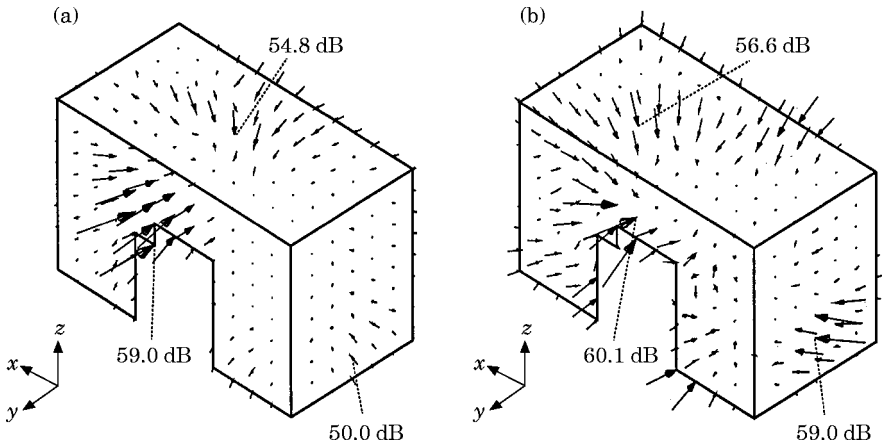

Figure 8. The sound intensity **I** on the measurement surface; 1624 Hz; levels of the maxima L_z in dB. (a) DtN–FEM; (b) experiment.

a good correspondence between measurement and calculation. There is also an acceptable agreement in the maximum level of the sound intensity vectors, which is mainly responsible for the level of the radiated power. The difference between the experiment and the numerical solution is only 1·1 dB. In this particular problem, the zone above the gap on the front side can be perceived to be a dominant source. The lid for the oil inlet on the top side of the gearbox can also be identified to be problematical with regard to acoustic effects.

6. CONCLUDING REMARKS

A finite element method for solving radiation problems of the Helmholtz equation in three dimensions has been presented. Calculations of the radiation of a breathing sphere show the good convergence of the method, especially for quadratic elements. The accuracy achieved is excellent. Its performance and ability are demonstrated for a real engineering problem. The results indicate that numerical simulations using finite elements with the DtN boundary condition are a good alternative to other methods in solving the reduced wave equation in infinite domains.

REFERENCES

1. D. Givoli 1988 *Ph.D. Thesis*, *Stanford University*. A finite element method for large domain problems.
2. J. Keller and D. Givoli 1989 *Journal of Computational Physics* **82**, 172–192. Exact non-reflecting boundary conditions.
3. I. Harari and T. J. R. Hughes 1991 *Computational Methods in Applied Mechanical Engineering* **87**, 59–96. Finite element methods for the Helmholtz equation in an exterior domain: model problems.
4. I. Harari and T. J. R. Hughes 1994 *International Journal for Numerical Methods in Engineering* **37**, 2935–2950. Studies of domain-based formulations for computing exterior problems of acoustics.
5. I. Harari and T. J. R. Hughes 1992 *Computational Methods in Applied Mechanical Engineering* **98**, 157–192. Galerkin/least-squares finite element methods for the reduced wave equation with non-reflecting boundary conditions in unbounded domains.
6. S. Vigdergauz and D. Givoli 1995 *Proceedings on Mathematical and Numerical Aspects on Wave Propagation*, 299–307. A finite element method for wave problems with geometrical singularities.
7. P. Bettess 1977 *International Journal for Numerical Methods in Engineering* **11**, 53–64. Infinite elements.
8. P. Bettess 1992 *Infinite Elements*. Sunderland: Penshaw Press.
9. F. G. Kollmann 1993 *Maschinenakustik*. Berlin: Springer-Verlag.
10. W. I. Smirnow 1964 *Lehrgang der höheren Mathematik*, *III*/2. Berlin: VEB Verlag der deutschen Wissenschaften.
11. T. J. R. Hughes 1987 *The Finite Element Method*. London: Prentice-Hall.
12. O. C. Zienkiewicz and R. L. Taylor 1989 *The Finite Element Method*. London: McGraw-Hill.
13. D. Givoli 1992 *Numerical Methods for Problems in Infinite Domains*. Amsterdam: Elsevier.
14. R. J. Astley 1996 *Communications in Numerical Methods in Engineering* **12**, 257–267. FE mode-matching schemes for the exterior Helmholtz problem and their relationship to the FE-DtN approach.
15. C. M. Piaszczyk and J. M. Klosner 1984 *Journal of the Acoustical Society of America* **75**(2), 363–375. Acoustic radiation from vibrating surfaces at characteristic frequencies.
16. K. A. Cunefare and G. H. Koopmann and K. Brod 1989 *Journal of the Acoustical Society of America* **85**(1), 39–48. A boundary element method for acoustic radiation valid for all wavenumbers.
17. M. Hoit and E. L. Wilson 1983 *Computers & Structures* **16**, 225–239. An equation numbering alogithm based on a minimum front criteria.

18. D. GILJOHANN 1996 *Ph.D. Thesis*, *TH Darmstadt*. Finite-Elemente-Methoden für die Schallabstrahlung ins Freifeld.
19. P. BETTESS and O. C. ZIENKIEWICZ 1977 *International Journal for Numerical Methods in Engineering* **11**, 1271–1290. Diffraction and refraction of surface waves using finite and infinite elements.
20. D. GILJOHANN and A. ZOPP *Journal of Vibration and Acoustics* (accepted for publication). Measurement of sound intensity in comparison with simulations using finite and semi-infinite Helmholtz-elements.